Supply Modulator Ripple in Envelope Tracking Systems - Effects and Countermeasures

Sattam Alsahali, Alexander Alt, Peng Chen, Guofeng Wang, Paul Tasker, Jonathan Lees
School of Engineering, Cardiff University, Cardiff, United Kingdom

***Abstract*— Envelope tracking power amplifiers (ET PAs) are one of the promising architectures to provide high efficiency amplification for future wireless communication systems. This is due to their ability to offer high efficiency over a wide output power range, by modulating the supply voltage applied to the PA. Generating this dynamic supply voltage with switching-mode modulators is highly efficient, but filtering the output remains a challenge, resulting in a residual 'ripple' on the supply voltage. This paper presents an experimental investigation into the interaction between a PA and a supply modulator in the presence of this ripple. By adding a varying ripple magnitude to the modulated drain voltage of a 2.14 GHz GaN ET PA with a 10 MHz LTE signal, the effects on the linearity of the RFPA can be observed and analysed to allow the system designer an insight into the amount of ripple that is tolerable, while still being able to achieve linearity and efficiency targets. The mixing products of the ripple and RF signal are shown to be a potential issue in ET PAs. This paper shows, for the first time, the full impact of the ripple voltage magnitude on the output spectrum.Further more, the ripple sensitivity of two different ET PA linearisation approaches are explored; firstly applying a generic memory polynomial digital pre-distortion (DPD) and secondly optimising the ET tracking signal shaping function to improve linearity. Measurements show that for the case where the ripple and RF are not synchronized, neither approach is able to significantly mitigate the ripple effect on the PA linearity.**

***Keywords*— Power amplifiers, Envelope tracking, ripple, supply modulator, linearity, efficiency, DPD.**

I. Introduction

Future generation communication systems will need to transfer data at much higher rates in comparison to existing systems, to accommodate the expected dramatic increase in mobile-cellular connectivity and wireless information exchange. To improve spectral efficiency, modulation schemes use signals with high peak-to-average power ratio (PAPR), leading to the substantial variation of the envelope magnitude of the modulated signal [1]. This dynamic variation in power distribution requires the conventional RFPA to operate under power back-off conditions, avoiding compression, which presents technical challenges in terms of achieving high linearity and back-off efficiency simultaneously [2]. To satisfy these requirements, several PA architectures have been proposed to improve the PA efficiency, such as and the Doherty PA [3] and envelope tracking [4], [5]. ET is a strong contender for both base transceiver station and user equipment applications due to its potential to support multimode and multiband operation. However, ET presents a number of technical challenges. The difficulty in ET system design and measurement is a consequence of the fact that an ET system comprises several subsystems: PA, envelope generation, supply modulator, and linearisation system. The supply modulator plays a vital role as it is a significant contributor to the overall performance of the ET PA in terms of modulation bandwidth, linearity, and overall efficiency. Despite a wide range of research focussing on supply modulator design [6]–[8], there are still significant challenges in achieving required performance in terms of modulation bandwidth, efficiency, and output voltage ripple, which limit the application of ET in commercial systems. Buck-converters are among the most efficient types of supply modulators but they inherently produce a significant ripple voltage. Filtering this ripple not only causes significant losses, especially through the use of high order filters [9], but also reduces the achievable modulation bandwidth at a given switching frequency. In this paper, the effects of voltage ripple [10]–[12] together with possible counter-measures [13] are explored and the impact of the ripple magnitude on an ET PA is quantified. In Section II, the theory behind the effect of ripple on a PA is introduced. Section III describes the measurement system and investigates the impact of different magnitudes of ripple on the PA linearity. The usual ways to linearise ET systems and their ability to minimize the effect of the ripple are discussed in Section IV.

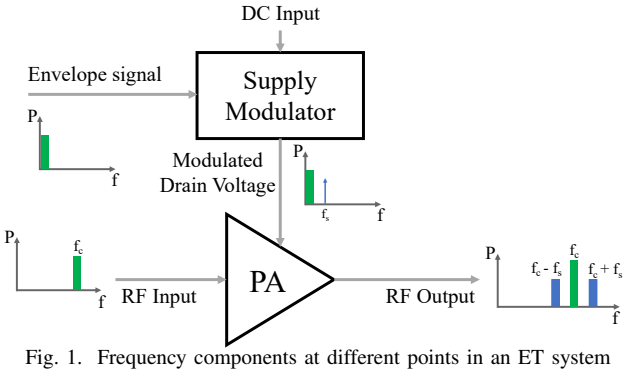

Fig. 1. Frequency components at different points in an ET system

II. Effect of Voltage Ripple on ET PAs - Theory

PAs achieve their highest efficiency when the applied drain voltage extends or swings to the lowest possible drain voltage, i.e. 0 in the case of an ideal transistor, and the knee region in a real device. Using signals with high PAPR, the PA is usually operated in output power back-off (OBO), i.e. operating at reduced output powers for most of the time in order to maintain good linearity. If the load impedance is fixed, a 6 dB reduction in output power will result in half the usual voltage swing, and a significant efficiency reduction. In envelope tracking, the PA

is maintained in an efficient mode of operation by dynamically changing the supply voltage in response to the modulation. In the same case of 6 dB OBO, the supply voltage is halved, thus restoring a maximum voltage swing and maintaining high efficiency. In the case of a real transistor, the function that generates the ET tracking voltage has to be carefully designed in order to prevent the device's dynamic load-line from intruding into the knee region, maintaining acceptable linearity [2]. As the ripple frequencies will be much lower

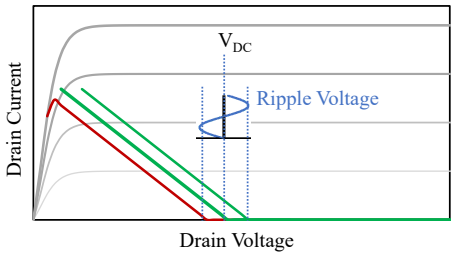

Fig. 2. Load line of an ideal class B PA effected by ripple voltage

than the RF frequency, the RF load-line can be assumed to be static during one RF period. The presence of ripple voltage superimposed onto the modulated supply voltage however, it will move the whole load-line along the voltage axis, alternating between moving the load-line towards the knee region, reducing the linearity, and away from the knee region, reducing the efficiency, see Fig. 2. The increased interaction with the knee region leads to increased non-linear behaviour of the PA, i.e. degradation in the error vector magnitude (EVM) and adjacent channel power ratio (ACPR). In addition to this linearity degradation, there is also a mixing effect taking place [10], up-converting the ripple to the side-bands around the carrier, with a separation entirely dependent on the ripple and its the switching frequency. A series analysis, assuming a memoryless system, delivers a first approximation of this mixing effect, see (1) [10]:

$$V_{out}(V_{in}, V_{ripple}) = \sum_{i,j=0}^{\infty} a_{i,j} {V_{in}}^i {V_{ripple}}^j \qquad (1)$$

where $a_{i,j}$ are the gain terms as a function of the ith order of the input voltage and the jth order of the voltage ripple, V_{out} is the output voltage, V_{in} and V_{ripple} are the input voltage and the output voltage ripple respectively. The first-order ripple-induced side-band will therefore be

$$V_{out}(t) = \tfrac{1}{2} a_{11} v_i v_r cos((\omega_0 \pm \omega_r)t) \qquad (2)$$

with $V_{in} = v_i cos(\omega_0 t)$ being the input voltage and $V_{ripple} = v_r cos(\omega_r t)$ being the output ripple.

III. Measurements

Fig. 3 illustrates the ET system that is used for the measurements in this paper, consisting of an National Instrument ET characterisation system supplemented with a supply modulator and an arbitrary waveform generator (AWG)) that generates the synthesised ripple voltage. The ripple and the modulated supply voltage are then combined using a bespoke diplexer consisting of a lumped low-pass filter and a lumped high-pass filter. The RFPA used in these measurements is designed using the Wolfspeed CGH40010F GaN HEMT, has a bandwidth of 100 MHz centred at 2.14 GHz and is biased in class AB. The PA is driven to its 1 dB compression point at peak envelope power (PEP). A two-stage supply modulator is realised using commercial operational amplifiers. The ripple frequency of 41 MHz is chosen so that the ripple-induced side-bands are within the frequency range around the carrier measured by the system but not too close to the PA's third and fifth order intermodulation side-bands. While the switching frequency in a real system would be higher for a 10 MHz modulation signal, the non-linear behaviour will be representative while keeping the ripple-induced side-bands well within the measurement bandwidth. A 10 MHz LTE

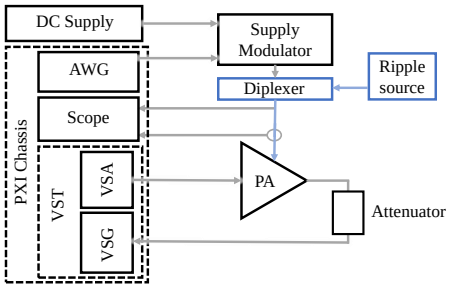

Fig. 3. Typical ET measurement system with extension for ripple measurement

signal with a PAPR of 6.8 dB is used as the RF modulation for all measurements. The envelope of the modulated signal is extracted from the IQ data in the NI system and shaped with the de-troughing shaping function (3) [14] to yield the desired envelope tracking drain bias voltage:

$$f(a) = V_{max}\left(1 - \left(1 - \frac{V_{min}}{V_{max}}\right) \cdot cos\left(a \cdot \frac{\pi}{2}\right)\right) \qquad (3)$$

where $f(a)$ is the modulated drain bias voltage, a is the normalised magnitude of the envelope of the input signal, V_{min} and V_{max} are the minimum and the maximum values for the drain bias voltage, respectively. The modulated drain voltage is time-aligned with the RF signal using the built-in delay optimiser and verified using the two-channel oscilloscope. For this PA, the minimum drain bias voltage is kept above

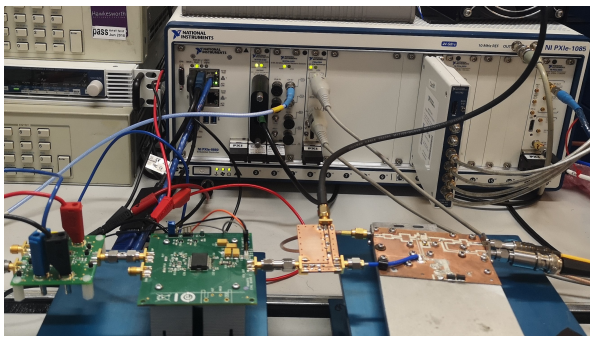

Fig. 4. Picture of the ET measurement setup

the knee voltage of approximately 8 V, the maximum is

set to 22 V as PA was designed as a test vehicle for a modulator with a maximum supply voltage of 22 V. The external ripple that is added to the drain bias voltage with a voltage amplitude increasing from 0 V to 2.2 V. The ripple voltage amplitude is normalized to the maximum voltage, see Fig. 5, with a maximum of 22 V this results in a normalised ripple magnitude, $\hat{v}_r$, between 0.02 and 0.1.

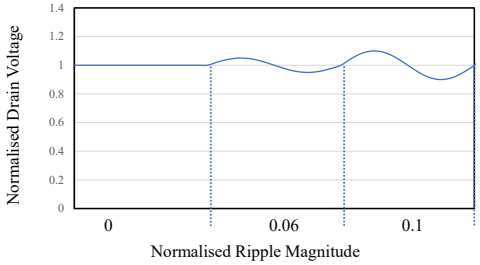

Fig. 5. Definition of the voltage normalisation

The linearity performance of the PA is determined by measuring the in-band and the out-of-band distortion in terms of EVM and ACPR, respectively. Fig. 6a shows that the EVM without ripple is 5.7%, and increase to 9.6% for a normalised ripple voltage $\hat{v}_r = 0.1$. The ACPR also suffers from increased ripple, increasing from -33.1 dBc with no injected ripple to -26.5 dBc when the normalized ripple amplitude reaches 0.1. Fig. 6b plots the measurements of the output spectrum of

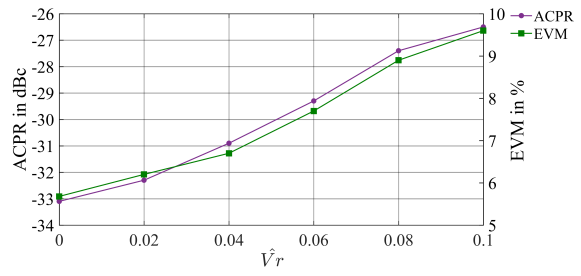

(a)

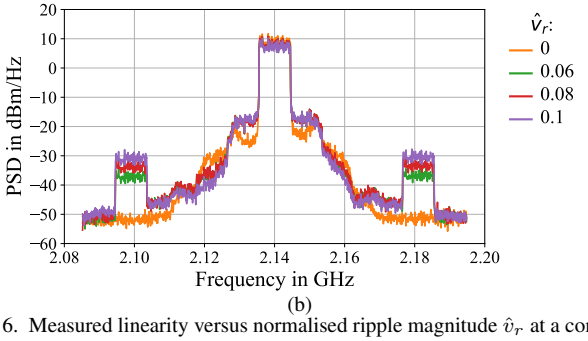

(b)

Fig. 6. Measured linearity versus normalised ripple magnitude $\hat{v}_r$ at a constant PEP and with no DPD: (a) EVM and ACPR (b) Power spectral density (PSD) at the PA output

the RFPA for different normalised ripple magnitudes. They illustrate the ACPR measurements in Fig. 6a, but the main point are the ripple induced side-bands. As expected, there are two additional side lobes separated from the carrier by the ripple frequency of 41 MHz, where their magnitude increases with the normalised ripple magnitude which is consistent with (2). This leads to two bands with a bandwidth of three times the modulation bandwidth each, separated from the carrier by the ripple frequency. In this experiment, the injected ripple was sinusoidal and thus only had one frequency component. Depending on the modulator topology and filter employed, the ripple voltage may have other shapes, e.g. triangular [13], which contain higher harmonic frequencies of the switching frequencies, additional side lobes at those higher harmonics should be expected to appear.

IV. Reducing Impact of Ripple

The two most common ways of linearising ET PAs are DPD and the use of optimised shaping functions [4], [5]. In this section, the usefulness of those two tools in reducing the ripple-induced non-linear behaviour is discussed. As DPD is already a part of most modern transmission systems, it could be argued that adding this new distortion, to the existing distortions generated through the 'normal' non-linearities of a PA, is not a problem as most of the non-linearity can be reduced at the same time. By applying a generalised

Table 1. Comparison of PA linearity with and without DPD

$\hat{v}_r$	DPD	EVM	$\text{ACPR}_{\text{high}}$	ACPR_{low}
0	No	5.7%	-33.1 dBc	-30.8 dBc
0	GMP	2.3%	-39.0 dBc	-38.5 dBc
0.1	No	9.6%	-26.5 dBc	-25.8 dBc
0.1	GMP	3.7%	-34.1 dBc	-35.5 dBc

memory polynomial (GMP), the in-band linearity can be dramatically improved, albeit not to the *non-ripple* levels. The real limitation of the DPD however is the out-band distortion: The ripple-induced side lobes are unchanged and the DPD introduces additional spurious trying to correct for those. As the ripple signal is not correlated with the RF signal, its relative phase keeps changing and it can not be predicted by the DPD. This also means that any attempt to pre-distort it is unsuccessful as long as ripple signal and RF are not coherent, an observation extending from previous work [13]. Another way of recovering the linearity is by modifying the

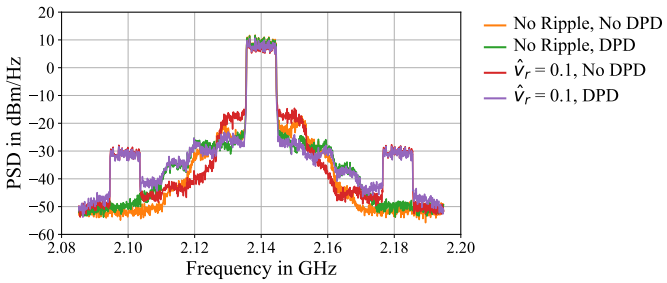

Fig. 7. Measured PSD at the PA output for cases with and without ripple and with and without DPD

shaping function. As shown in Fig. 2, the dynamic load line at PEP drops into the knee region by the ripple voltage. Theoretically, this knee region interaction can be prevented

by shifting the supply voltage away from the knee, moving the ripple voltage with it, see Fig. 8. By doing so, the drain voltage never goes below the un-shifted, ripple-free case. This shift in supply voltage comes at the cost of efficiency however, as the mean drain voltage is now increased by the ripple voltage magnitude, see Fig. 8. The shift in supply

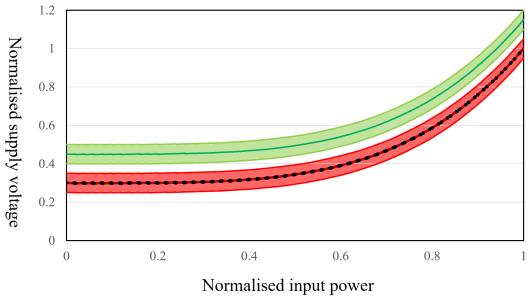

Fig. 8. Diagram showing the minimum voltage required to keep the PA load-line out of the knee region (black, dotted), the unmodified shaping function (dark red, the red area highlights the voltage range covered by the ripple) and an shifted shaping function (dark green, the green area highlights the voltage range covered by the ripple)

Table 2. Comparison of PA linearity for different levels of voltage shift

$\hat{v}_r$	Voltage Shift	EVM	$\text{ACPR}_{\text{high}}$	ACPR_{low}	PAE
0.1	0 V	9.6%	-26.4 dBc	-25.8 dBc	35.3%
0.1	1 V	7.4%	-29.5 dBc	-28.5 dBc	34.1%
0.1	2 V	6.2%	-32.3 dBc	-30.8 dBc	32.1%
0.1	3 V	5.5%	-33.9 dBc	-32.6 dBc	31.7%

voltage does significantly improve the in-band linearity while reducing the PAE. Even small levels of voltage elevation lead to significant improvements, showing an opportunity of trading off linearity and PAE. The magnitude of the ripple-induced

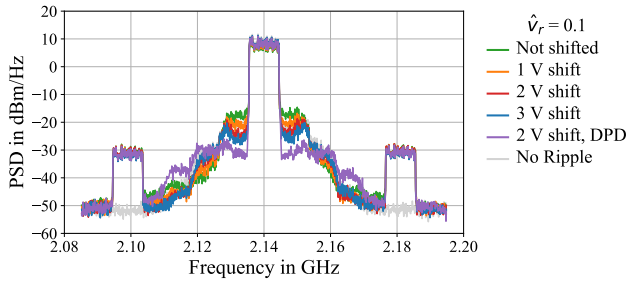

Fig. 9. Measured PSD at the PA output for different levels of envelope voltage shift

side-bands however is not reduced significantly, see Fig. 9. Even a combination of voltage shift and DPD is not sufficient to recover the out-of-band non-linearities that are introduced by the mixing process.

V. Conclusion

In this paper, the effects of supply voltage ripple on the linearity of the ETPA is presented. It is first discussed theoretically, considering the output ripple effect on the linearity of the ETPA. The measured results confirm theory, showing that linearity degrades as the ripple amplitude increases. Importantly, it is shown that the usefulness of digital pre-distortion (DPD) linearisation is limited when significant non-coherent output ripple is present, due to the unpredictable nature of the interaction between the load-line and knee region. Reshaping the drain bias voltage by adapting the shaping function can reduce the knee region interaction, and thus enhances the linearity performance albeit at the cost of efficiency. It is however not able to correct the side-band introduced by the mixing between ripple and RF, even when combined with DPD.

Acknowledgement

This work was supported by the Engineering and Physical Science Research Council (EPSRC), UK, in the context of the research project EP/N016408/1. The authors would like to thank the Saudi Arabia Cultural Bureau in London for their support.

References

[1] E. McCune, *Dynamic Power Supply Transmitters*. Cambridge University Press, 2015, Cambridge Books Online.

[2] S. Cripps, *RF Power Amplifiers for Wireless Communications*. Artech House, 2006.

[3] V. Camarchia, M. Pirola, R. Quaglia, S. Jee, Y. Cho, and B. Kim, "The Doherty Power Amplifier: Review of Recent Solutions and Trends," *IEEE Trans. Microw. Theory Techn.*, vol. 63, no. 2, pp. 559–571, Feb. 2015.

[4] Z. Popović, "GaN power amplifiers with supply modulation," in *IEEE MTT-S Int. Microw. Symp. Dig.*, May 2015, pp. 1–4.

[5] B. Kim, J. Kim, D. Kim, J. Son, Y. Cho, J. Kim, and B. Park, "Push the Envelope: Design Concepts for Envelope-Tracking Power Amplifiers," *IEEE Microwave Magazine*, vol. 14, no. 3, pp. 68–81, May 2013.

[6] N. Wolff, W. Heinrich, and O. Bengtsson, "100 MHz GaN HEMT Class G Supply Modulator for High-Power Envelope-Tracking Applications," *IEEE Trans. Microw. Theory Techn.*, vol. 65, no. 3, pp. 872–880, Mar. 2017.

[7] P. Theilmann, J. Yan, C. Vu, J.-S. Moon, H. Moyer, and D. Kimball, "A 60MHz Bandwidth High Efficiency X-Band Envelope Tracking Power Amplifier," in *Compound Semiconductor Integrated Circuit Symposium (CSICS), 2013 IEEE*, Oct. 2013, pp. 1–4.

[8] A. Disserand, A. Martin, P. Bouysse, and R. Quéré, "High efficiency GaN HEMT switching device with integrated driver for envelope tracking modulators," in *2018 International Workshop on Integrated Nonlinear Microwave and Millimetre-wave Circuits (INMMIC)*, Jul. 2018, pp. 1–3.

[9] S. Paul, N. Wolff, C. Delepaut, V. Valenta, W. Heinrich, and O. Bengtsson, "Analysis of Dissipated Power in Envelope Amplifier Output Filters," in *2018 48th European Microwave Conference (EuMC)*, 2018, pp. 515–518.

[10] J. T. Stauth and S. R. Sanders, "Power Supply Rejection for RF Amplifiers: Theory and Measurements," *IEEE Trans. Microw. Theory Techn.*, vol. 55, no. 10, pp. 2043–2052, 2007.

[11] M. Hassan, L. Larson, V. Leung, and P. Asbeck, "Effect of envelope amplifier nonlinearities on the output spectrum of Envelope Tracking Power Amplifiers," in *Silicon Monolithic Integrated Circuits in RF Systems (SiRF), 2012 IEEE 12th Topical Meeting on*, Jan. 2012, pp. 187–190.

[12] B. Sahu and G. A. Rincon-Mora, "System-level requirements of DC-DC converters for dynamic power supplies of power amplifiers," in *Proceedings. IEEE Asia-Pacific Conference on ASIC,*, 2002, pp. 149–152.

[13] H. Kobayashi and P. M. Asbeck, "Active cancellation of switching noise for DC-DC converter-driven RF power amplifiers," in *IEEE MTT-S Int. Microw. Symp. Dig.*, vol. 3, 2002, 1647–1650 vol.3.

[14] Rohde & Schwarz, "Envelope Tracking and Digital Pre-Distortion Test Solution for RF Amplifiers," Tech. Rep., 2017.